Engineering Spin-Orbit Synthetic Hamiltonians in Liquid Crystal Optical Cavities

Katarzyna Rechcińska[1], Mateusz Król[1], Rafał Mazur[2], Przemysław Morawiak[2], Rafał Mirek[1], Karolina Łempicka[1], Witold Bardyszewski[3], Michał Matuszewski[4], Przemysław Kula[5], Wiktor Piecek[2], Pavlos G. Lagoudakis[6,7,*], Barbara Piętka[1], and Jacek Szczytko[1,†]

[1]Institute of Experimental Physics, Faculty of Physics, University of Warsaw, Poland
[2]Institute of Applied Physics, Military University of Technology, Warsaw, Poland
[3]Institute of Theoretical Physics, Faculty of Physics, University of Warsaw, Poland
[4]Institute of Physics, Polish Academy of Sciences, al. Lotników 32/46, PL-02-668 Warsaw, Poland
[5]Institute of Chemistry, Military University of Technology, Warsaw, Poland
[6]Department of Physics and Astronomy, University of Southampton, Southampton SO17 1BJ, UK
[7]Skolkovo Institute of Science and Technology, Moscow, Russian Federation
[*]p.lagoudakis@skoltech.ru
[†]jacek.szczytko@fuw.edu.pl

Spin-orbit interactions lead to novel functionalities in photonic systems. They exploit the analogy between the quantum mechanical description of a complex electronic spin-orbit system and synthetic Hamiltonians derived for the propagation of electromagnetic waves in dedicated spatial structures. We realize an artificial Rashba-Dresselhaus spin-orbit interaction in a liquid-crystal-filled optical cavity. Three-dimensional tomography in energy-momentum space enables us to directly evidence the spin-split photon mode in the presence of an artificial spin-orbit coupling. The effect is observed when two orthogonal linear polarized modes of opposite parity are brought near resonance. Engineering of spin-orbit synthetic Hamiltonians in optical cavities opens the way to photonic emulators of quantum Hamiltonians with internal degrees of freedom.

Spin-orbit interaction (SOI) in atomic and solid state physics is a relativistic effect transforming static electric fields in the laboratory frame into magnetic fields in the frame of a moving electron. These magnetic fields interact with the spin of the electron and result in a rich variety of quantum phenomena including the realization of topological states (*1*). SOI in solid-state systems with broken inversion symmetries leads to the so-called Dresselhaus (*2*) and Bychkov-Rashba (*3*, *4*) Hamiltonians that underpin device concepts in spintronics, topological insulators, and superconductors (*5*). SOI effects of light stem directly from the solutions of Maxwell equations in wavelength-scale micro- and nano-structures, including metamaterials, optical waveguides and interfaces (*6*–*14*), where the role of spin is taken by the polarization of the photons. In the case of a homogeneous medium enclosed in a microcavity, the presence of an energy splitting between transverse electric (TE) and transverse magnetic (TM) modes of light leads to the optical analogue of the spin Hall effect (*15*, *16*) and the realization of artificial gauge fields (*17*, *18*).

The Hamiltonian of a charged particle in a magnetic field is known to be simulated by certain photonic systems with induced gauge fields (*19*–*22*). In these devices the vector potentials describing the gauge fields are spin-independent and so the particle's internal degree of freedom remains unaffected. The coupling between potential and spin has been realized, e.g., in metamaterials (*23*, *24*). However, the study of artificial Rashba-Dresselhaus spin-orbit gauge fields has been so far predominantly restricted to nano-Kelvin temperatures in atomic systems (*25*, *26*).

In this Report, we simulate spin-orbit interactions in a tuneable, liquid crystal (LC) filled, optical cavity. By controlling the refractive index anisotropy of the intra-cavity layer, we adiabatically engineer the coupling between optical modes, and show that the system is described by a Hamiltonian with Dresselhaus (*2*) and Bychkov-Rashba (*3*, *4*) terms, originally used to describe fermions. We fabricate a 2D capacitive planar multi-mode optical cavity and fill it with a birefringent LC medium in the nematic state, as shown in Fig. 1A (*27*). By applying an external voltage, we control the spatial orientation of the long molecular axis of the LC medium that induces refractive index anisotropy. The refractive index anisotropy in the xy plane can be described using ordinary n_{o} and extraordinary n_{e} refractive indices. At normal incidence, for a cavity mode with l anti-nodes, this leads to an energy splitting between the two orthogonal linearly polarized cavity modes, with energies denoted by $E_{X,l}$ and $E_{Y,l}$. By rotating the optical axis of the LC medium around the y-axis, shown in Fig.1A, we control the effective refractive index relevant to the electric field oscillating in the xz-plane, and thus the energy of the X-polarized modes (*28*). This configura-

tion enables us to utilize the giant optical anisotropy of the LC medium [$\Delta n = n_e - n_o = 0.41$ (*29*)] and bring successive modes into resonance.

When two orthogonally polarized cavity modes of opposite parity of the number of antinodes l and l' are tuned near resonance, a coupling between them arises, which depends on the in-plane wavevector of incident light, denoted as $\mathbf{k}_\parallel = (k_x, k_y)$. The coupling term is analogous to the Rashba-Dresselhaus Hamiltonian with equal strength of Rashba and Dresselhaus couplings (*30*), $\hat{H}_{R\text{-}D} = -2\alpha\hat{\sigma}_z k_y$, where $\hat{\sigma}_z$ is the third Pauli matrix, (defined in the basis of circular polarizations of out-coupled light $\sigma^\pm$ at the LC, Bragg mirror interface, shown in Fig. 1B), and α is the Rashba-Dresselhaus coupling coefficient. This form of the Rashba-Dresselhaus coupling term can be deduced from the symmetry of the system (*27*).

The quasi-degenerate system of the orthogonally polarized modes of opposite parity can be approximately described by the effective Hamiltonian

$$\hat{H} = \frac{\hbar^2 k_x^2}{2m_x} + \frac{\hbar^2 k_y^2}{2m_y} + \hat{H}_{R\text{-}D} + \frac{1}{2}(E_{X,l} - E_{Y,l'})\hat{\sigma}_x, \quad (1)$$

where m_x and m_y are the effective masses of the cavity photon in the xy-plane, cf. Fig. 1A. The first two terms correspond to the kinetic energy of cavity photons i.e. photon confinement in the z-direction results in a parabolic dispersion relation with respect to $\mathbf{k}_\parallel$ i.e. the photon in-plane momentum. The third term corresponds to the Rashba-Dresselhaus coupling with a gauge field defined as $\hat{\mathbf{A}} = 2m_y\hat{\sigma}_z/\hbar\,(0,1,0)$. The Rashba-Dresselhaus coupling gives rise to two cross-circular polarised eigenstates separated in momentum space, shown in Fig. 1C. Constant energy cross-sections of the 3D parabolloid are shown in Fig. 1D. The last term in Hamiltonian (1) corresponds to the splitting between the cavity eigenmodes $E_{X,l}$ and $E_{Y,l'}$ that acts as an artificial magnetic field in the x-direction resulting in a synthetic Zeeman term for the spin but not the orbital degree of freedom (*31*).

Under oblique incidence, the eigenmodes are neither X- nor Y-polarized since $\mathbf{k}_\parallel \neq 0$. At resonance the phase difference between the X- and Y-polarisation modes across the intracavity LC layer changes by π. The intracavity LC layer acts then as a half-wave plate and the eigenmode polarization at the mirror interfaces becomes circular, and thus out-coupled light is circularly $\sigma^\pm$ polarized, with the same polarization on both sides of the cavity, as shown in Fig. 1B.

The lifted degeneracy of $\sigma^\pm$ polarizations (Fig. 1C) and the asymmetric cross-section in reciprocal-space (Fig. 1D) of the Rashba-Dresselhaus coupled photons appear to break time reversal (TR) symmetry in a purely photonic system. Paradoxically, the possibility to realize synthetic Rashba-Dresselhaus spin-orbit coupling for photons in such a simple system can be precisely justified by considering the effect of TR symmetry on confined photon modes. As shown in Fig. 1E, TR of a ($\mathbf{k}$,$\sigma^\pm$) circularly polarized electromagnetic wave in free space results in an electromagnetic wave with opposite momentum $-\mathbf{k}$ and the same polarization. Consequently, in a TR symmetric system a plane wave spectrum is always symmetric with respect to inversion of momentum $\mathbf{k}$. However, such symmetry argument does not hold for cavity modes parameterized with momentum in the plane of the cavity because ($\mathbf{k}_\parallel$,$\sigma^\pm$) and ($-\mathbf{k}_\parallel$,$\sigma^\pm$) are not TR symmetric partners. Indeed, reflection of circularly polarised light flips both the sign of the component of the wavevector perpendicular to the mirror, $\mathbf{k}_\perp$, and the polarization, $\sigma^\mp$, as shown schematically in Fig. 1F,G. Therefore, modes ($\mathbf{k}_\parallel$,$\mathbf{k}_\perp$,$\sigma^\pm$) and ($\mathbf{k}_\parallel$,$-\mathbf{k}_\perp$,$\sigma^\mp$), couple in the cavity and form a standing wave. Thus TR in the cavity transforms ($\mathbf{k}_\parallel$,$\mathbf{k}_\perp$,$\sigma^\pm$) into ($-\mathbf{k}_\parallel$,$\mathbf{k}_\perp$,$\sigma^\mp$), i.e. $\mathbf{k}_\parallel \to -\mathbf{k}_\parallel$ and $\sigma^\pm \to \sigma^\mp$. This permits asymmetric spectra in both $\sigma^\pm$ polarizations that result into the apparent symmetry "breaking" with respect to $\mathbf{k} = 0$, reminiscent to that of fermionic spin-1/2 particles (*27*).

To experimentally realise the manifestation of the Rashba-Dresselhaus coupling, we perform polarisation resolved reflectivity measurements in reciprocal-space. We use a broadband incoherent source, to eliminate coherent artifacts. In the absence of an external voltage (first row of Fig.2), the director of the LC medium is parallel to the cavity plane, pointing in the x-direction. In this configuration, we expect a large energy splitting between the X-, Y-polarisation modes. The 2D polarisation resolved dispersion of the cavity photons consists of coaxial paraboloids shown in Fig. 2A, where we can clearly observe two successive cavity modes. Fig. 2B shows the corresponding reflectivity dispersion at the $k_x = 0$ cross-section. Polarisation resolved reflectivity of the dispersion along the X- and Y-polarisation modes, allows us to distinguish the relevant modes. Fig. 2C shows the dispersion of the Degree of Linear Polarisation (DLP) at the $k_x = 0$ cross-section of the 2D dispersion. The two orthogonal modes corresponds to the main axes of the LC indicatrix.

Application of an external voltage on the electrodes of the cavity allows for a smooth tuning of the energy of the X-polarised paraboloid. At 1.38 V, two orthogonally polarized modes of the same parity are brought into a resonance at normal incidence (second row of Fig.2). Fig. 2D shows the 2D polarisation resolved dispersion, and Fig. 2E shows the corresponding reflectivity dispersion at the $k_x = 0$ cross-section. The two modes have slightly different curvature (effective masses) in the k_y-direction due to the residual alignment of the LC director; naturally the cross-section at k_x-direction (left projection of Fig. 2D) does not exhibit any difference. The dispersion of the degree of linear polarisation at the $k_x = 0$ cross-section of the 2D dispersion, shown

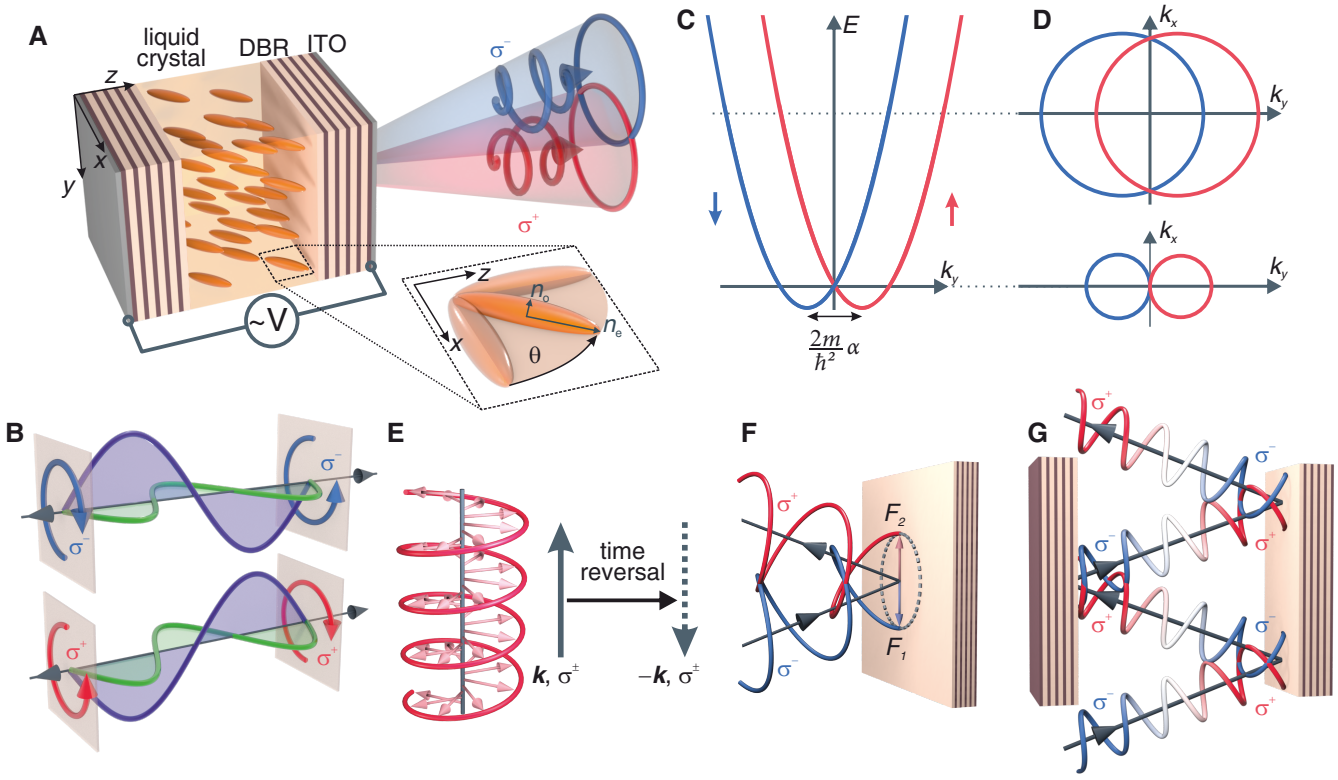

Figure 1. Rashba–Dresselhaus spin-orbit coupling in a liquid-crystal-filled optical cavity. A Scheme of the liquid crystal (LC) filled optical cavity and its coordinates. **B** Resonant $X-$ and $Y-$polarisation modes of opposite parities l,l'; the LC medium acts as a half-wave plate and the eigenmode polarization at the mirror interfaces becomes circular. Out-coupled light is circularly polarised with the same ($\sigma^{\pm}$) polarization on either side of the cavity. **C** Dispersion relation with spin-polarised bands resulting from Rashba–Dresselhaus coupling. **D** Constant energy cross-sections in k_{xy} reciprocal space. **E** Circularly polarized beam under time-reversal (TR) switches its propagation direction, but the chirality remains the same. In a TR symmetric system, this results in **k**-symmetric spectra for all polarisations. **F** Mirror reflection switches both the perpendicular part of the momentum and the chirality of the incident beam. **G** In the cavity, both ($\mathbf{k}_{\parallel}$,$\mathbf{k}_{\perp}$,$\sigma^{\pm}$) and ($\mathbf{k}_{\parallel}$,$-\mathbf{k}_{\perp}$,$\sigma^{\mp}$) modes couple with each other to form a standing wave. Under TR both wavevector parallel to the cavity plane and circular polarisation change sign, $\mathbf{k}_{\parallel} \to -\mathbf{k}_{\parallel}$ and $\sigma^{\pm} \to \sigma^{\mp}$, resulting in symmetry breaking of the intracavity circularly polarized modes.

in Fig. 2F, reveals that the two modes maintain their polarisation.

For an even higher external bias of 2.48 V, we bring into resonance two orthogonally polarised modes of opposite parity (third row of Fig.2). Fig. 2G shows the 2D polarisation resolved dispersion, analysed in the circular polarisation basis. Here, we observe a clear splitting of the paraboloids in the k_y-direction. Fig. 2H shows the corresponding reflectivity dispersion at the $k_x = 0$ cross-section. The dispersion of the degree of circular polarisation (DCP) at the $k_x = 0$ cross-section of the 2D dispersion, shown in Fig. 2I, reveals the Rashba-Dresselhaus Hamiltonian solution of Fig. 1C.

The emergence of the coupling between the modes can be precisely traced on the reflectivity dispersion as a function of the applied voltage. In Fig. 3A we plot the reflectivity spectrum vs applied voltage at normal incidence ($k_y = 0$) for the range of voltages, wherein we observe crossing of the resonances of two orthogonal polarisation modes with opposite parity. At normal incidence, we observe a clear crossing of the two modes, in agreement with the Rashba-Dresselhaus coupling term. In Fig. 3B we plot the reflectivity spectrum vs applied voltage at $k_y = 1.4\,\mu\text{m}^{-1}$. In this case, we observe a clear anti-crossing at the resonance conditions for the two modes. This is in agreement with the Rashba-Dresselhaus coupling term that is linear on in-plane wavevector (k_y). Tuning the applied voltage we determined the splitting as a function of the wave vectors (Fig. 3C). From the slope of the linear dependence of the energy splitting on k_y, we obtain a giant Dresselhaus-Rashba parameter of $\alpha = 31.9\,\text{eV}\cdot\text{Å}$.

We demonstrate a photonic device that realises a tuneable synthetic Hamiltonian consisting of the Rashba-

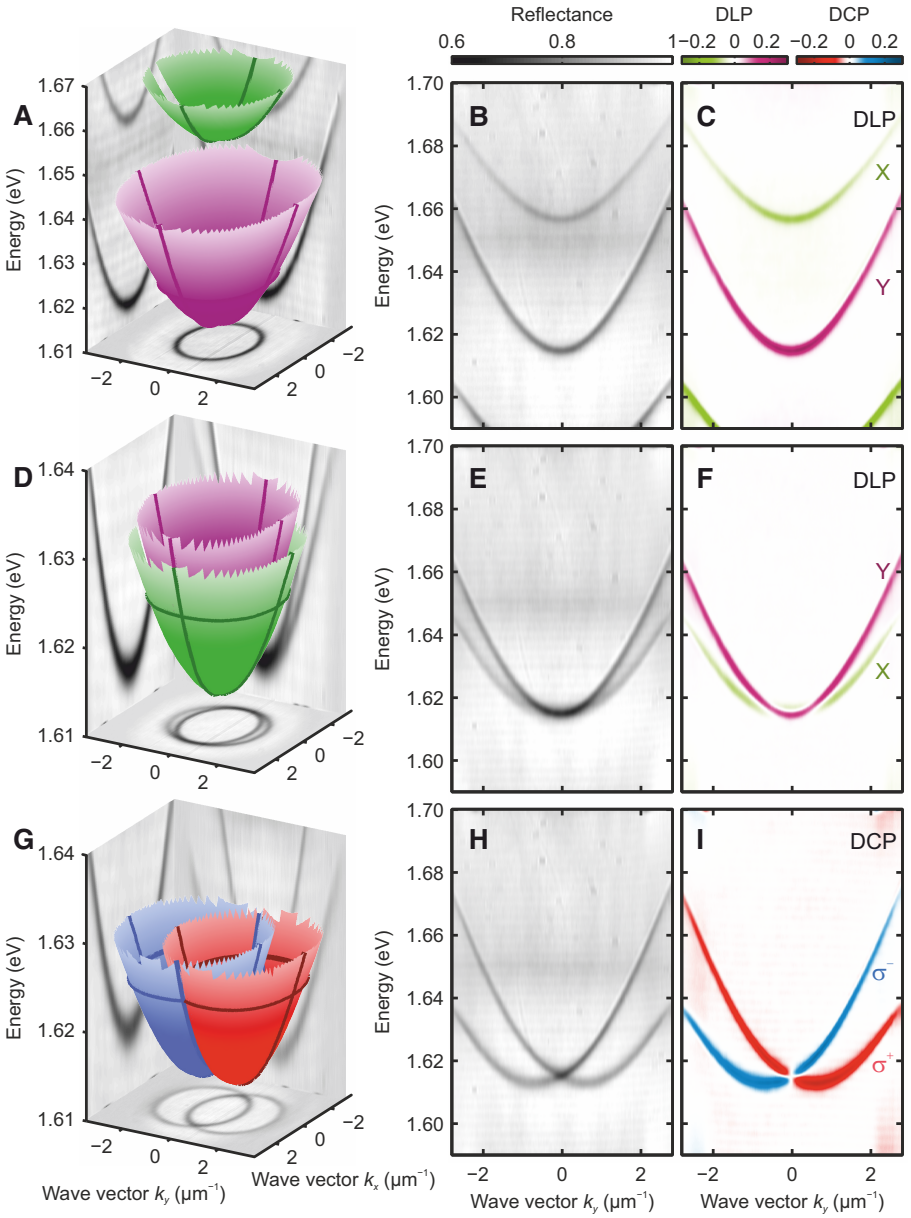

Figure 2. Dispersion engineering in a tunable liquid-crystal-filled optical cavity. A, D, G Experimental 2D polarisation resolved, reciprocal space tomography of reflectance at 0.0 V, 1.38 V and 2.48 V respectively. **B, E, H** Reflectance dispersion at the $k_x = 0$ cross-section. **C, F** The dispersion of the degree of linear polarisation (DLP) at the $k_x = 0$ cross-section of the respective 2D dispersions for modes of the same parity. The two orthogonal modes corresponds to the main axes of the LC indicatrix. **I** The dispersion of the degree of circular polarisation (DCP) at the $k_x = 0$ cross-section of the 2D dispersion realising the solution of the Rashba-Dresselhaus Hamiltonian of Fig. 1C.

Dresslehauss and Zeeman terms. Synthetic Hamiltonians enable the study of physical systems, wherein tuneable gauge fields and forces play an important role. Utilising pure bosons to engineer the Rashba-Dresselhaus Hamiltonian allows for the emulation of physical systems with SOI and microscale control over spin states e.g. persistent spin helix (*30*), suppression of spin relaxation (*32*) and creation of topologically protected states of light (*33*). Such artificial gauge fields can be further applied to light-matter dressed-states bringing about exotic Hamiltonian with instrinsic non-linearities.

Acknowledgments: This work was supported by the Ministry of Higher Education, Poland, under project "Diamentowy Grant": 0005/DIA/2016/45 and 0109/DIA/2015/44, the National Science Centre grants 2016/23/B/ST3/03926, 2016/22/E/ST3/00045,

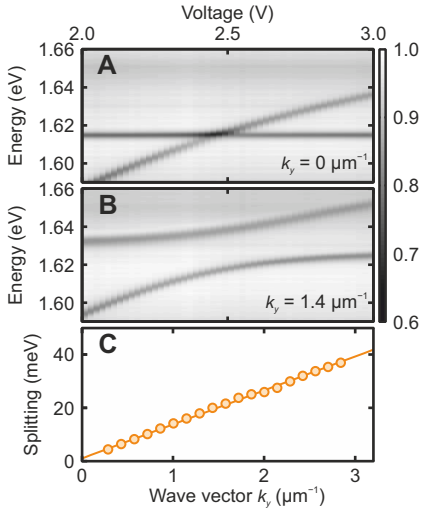

Figure 3. Giant Rashba coupling in an optical cavity. A,B Reflectance at $k_y = 0$ and $k_y = 1.4\,\mu\text{m}^{-1}$ respectively vs applied voltage. **C** Energy mode splitting between the cavity eigenmodes $E_{X,l}$ and $E_{Y,l'}$ vs in-plane wavevector k_y at 2.48 V. From the slope of a linear fit to the data we obtain a giant Rashba -Dresselhaus parameter of $\alpha = 31.9\,\text{eV}\cdot\text{Å}$.

2017/27/B/ST3/00271 and 2018/31/N/ST3/03046 and the Ministry of National Defense Republic of Poland Program – Research Grant MUT Project 13–995, UK Engineering and Physical Sciences Research Council grant EP/M025330/1 on Hybrid Polaritonics.

Author contributions: KR and MK contributed equally to this work. K.R., M.K., R.Mi. and K.Ł., performed the experiments with B.P. and J.S. guidance. P.K. synthesized liquid crystal. R.Ma., P.M., and W.P. constructed and fabricated the LCMC. M.M. worked on the theoretical description. W.B. developed the waveguide approximation. M.M. determined polarizations on the Poincare sphere. All authors participated in the interpretation of experimental data. J.S., BP and P.G.L supervised the project. P.G.L., J.S., M.K. and K.R. wrote the manuscript with input from all other authors. **Competing interests:** Authors declare no competing interests.

Data and materials availability: All data is available in the main text or the supplementary materials.

References

1. M. Z. Hasan, C. L. Kane, Colloquium: Topological insulators. *Rev. Mod. Phys.* **82**, 3045 (2010). doi:10.1103/RevModPhys.82.3045
2. G. Dresselhaus, Spin-orbit coupling effects in zinc blende structures. *Phys. Rev.* **100**, 580 (1955). doi:10.1103/PhysRev.100.580
3. E. I. Rashba, V. I. Sheka, Simmetriya energeticheskikh zon v kristallakh tipa vyurtsita. II. Simmetriya zon s uchyotom spinovykh vzaimodeistvii. *Fiz. Tverd. Tela: Collected Papers* **2**, 162 (1959)
4. Y. A. Bychkov, E. Rashba, Properties of a 2D electron gas with lifted spectral degeneracy. *JETP Lett.* **39**, 78 (1984)
5. A. Manchon, H. C. Koo, J. Nitta, S. M. Frolov, R. A. Duine, New perspectives for Rashba spin-orbit coupling. *Nat. Mater.* **14**, 871 (2015). doi:10.1038/nmat4360
6. V. S. Liberman, B. Y. Zel'dovich, Spin-orbit interaction of a photon in an inhomogeneous medium. *Phys. Rev. A* **46**, 5199 (1992). doi:10.1103/PhysRevA.46.5199
7. K. Y. Bliokh, F. J. Rodríguez-Fortuño, F. Nori, A. V. Zayats, Spin-orbit interactions of light. *Nat. Photonics* **9**, 796 (2015). doi:10.1038/nphoton.2015.201
8. F. Cardano, L. Marrucci, Spin-orbit photonics. *Nat. Photonics* **9**, 776 (2015). doi:10.1038/nphoton.2015.232
9. K. Y. Bliokh, Geometrodynamics of polarized light: Berry phase and spin Hall effect in a gradient-index medium. *Journal of Optics A: Pure and Applied Optics* **11**, 094009 (2009). doi:10.1088/1464-4258/11/9/094009
10. K. Y. Bliokh, D. Smirnova, F. Nori, Quantum spin Hall effect of light. *Science* **348**, 1448 (2015). doi:10.1126/science.aaa9519
11. M. Onoda, S. Murakami, N. Nagaosa, Hall effect of light. *Phys. Rev. Lett.* **93**, 083901 (2004). doi:10.1103/PhysRevLett.93.083901
12. K. Y. Bliokh, Y. Gorodetski, V. Kleiner, E. Hasman, Coriolis effect in optics: Unified geometric phase and spin-Hall effect. *Phys. Rev. Lett.* **101**, 030404 (2008). doi:10.1103/PhysRevLett.101.030404
13. A. Aiello, N. Lindlein, C. Marquardt, G. Leuchs, Transverse angular momentum and geometric spin Hall effect of light. *Phys. Rev. Lett.* **103**, 100401 (2009). doi:10.1103/PhysRevLett.103.100401
14. K. Y. Bliokh, C. Prajapati, C. T. Samlan, N. K. Viswanathan, F. Nori, Spin-hall effect of light at a tilted polarizer. *Opt. Lett.* **44**, 4781 (2019). doi:10.1364/OL.44.004781
15. A. Kavokin, G. Malpuech, M. Glazov, Optical spin Hall effect. *Phys. Rev. Lett.* **95**, 136601 (2005). doi:10.1103/PhysRevLett.95.136601
16. C. Leyder, M. Romanelli, J. P. Karr, E. Giacobino, T. C. H. Liew, M. M. Glazov, A. V. Kavokin, G. Malpuech, A. Bramati, Observation of the optical spin Hall effect. *Nat. Phys.* **3**, 628 (2007). doi:10.1038/nphys676

17. H. Terças, H. Flayac, D. D. Solnyshkov, G. Malpuech, Non-abelian gauge fields in photonic cavities and photonic superfluids. *Phys. Rev. Lett.* **112**, 066402 (2014). doi:10.1103/PhysRevLett.112.066402

18. A. Gianfrate, O. Bleu, Direct measurement of the quantum geometric tensor in a two-dimensional continuous medium. arXiv:1901.03219v1. [cond-mat.mes-hall] (10 Jan 2019)

19. M. Aidelsburger, S. Nascimbene, N. Goldman, Artificial gauge fields in materials and engineered systems. *C. R. Physique* **19**, 394 (2018). doi:10.1016/j.crhy.2018.03.002

20. H.-T. Lim, E. Togan, M. Kroner, J. Miguel-Sanchez, A. Imamoglu, Electrically tunable artificial gauge potential for polaritons. *Nat. Commun.* **8**, 14540 (2017). doi:10.1038/ncomms14540

21. Z. Wang, Y. Chong, J. D. Joannopoulos, M. Soljacic, Observation of unidirectional backscattering-immune topological electromagnetic states. *Nature* **461**, 772 (2009). doi:10.1038/nature08293

22. M. C. Rechtsman, J. M. Zeuner, A. Tünnermann, S. Nolte, M. Segev, A. Szameit, Strain-induced pseudomagnetic field and photonic Landau levels in dielectric structures. *Nat. Photonics* **7**, 153 (2012). doi:10.1038/nphoton.2012.302

23. N. Shitrit, I. Yulevich, E. Maguid, D. Ozeri, D. Veksler, V. Kleiner, E. Hasman, Spin-optical metamaterial route to spin-controlled photonics. *Science* **340**, 724 (2013). doi:10.1126/science.1234892

24. Y. Lumer, M. A. Bandres, M. Heinrich, L. J. Maczewsky, H. Herzig-Sheinfux, A. Szameit, M. Segev, Light guiding by artificial gauge fields. *Nat. Photonics* **13**, 339 (2019). doi:10.1038/s41566-019-0370-1

25. Y.-J. Lin, K. Jiménez-García, I. B. Spielman, Spin-orbit-coupled Bose-Einstein condensates. *Nature* **471**, 83 (2011). doi:10.1038/nature09887

26. V. Galitski, I. B. Spielman, Spin-orbit coupling in quantum gases. *Nature* **494**, 49 (2013). doi:10.1038/nature11841

27. See supplementary materials.

28. K. Lekenta, M. Król, R. Mirek, K. Lempicka, D. Stephan, R. Mazur, P. Morawiak, P. Kula, W. Piecek, P. G. Lagoudakis, B. Pietka, J. Szczytko, Tunable optical spin Hall effect in a liquid crystal microcavity. *Light Sci. Appl.* **7**, 74 (2018). doi:10.1038/s41377-018-0076-z

29. E. Miszczyk, R. Mazur, P. Morawiak, M. Mrukiewicz, W. Piecek, Z. Raszewski, P. Kula, K. Kowiorski, J. Kędzierski, J. Zieliński, Refractive index matched liquid crystal cell for laser metrology application. *Liquid Crystals* **45**, 1690 (2018). doi:10.1080/02678292.2018.1471745

30. B. A. Bernevig, J. Orenstein, S.-C. Zhang, Exact SU(2) symmetry and persistent spin helix in a spin-orbit coupled system. *Phys. Rev. Lett.* **97**, 236601 (2006). doi:10.1103/PhysRevLett.97.236601

31. D. Solnyshkov, G. Malpuech, Chirality in photonic systems. *C. R. Physique* **17**, 920 (2016). doi:10.1016/j.crhy.2016.07.003

32. J. D. Koralek, C. P. Weber, J. Orenstein, B. A. Bernevig, S.-C. Zhang, S. Mack, D. D. Awschalom, Emergence of the persistent spin helix in semiconductor quantum wells. *Nature* **458**, 610 (2009). doi:10.1038/nature07871

33. D. Leykam, K. Y. Bliokh, C. Huang, Y. D. Chong, F. Nori, Edge modes, degeneracies, and topological numbers in non-Hermitian systems. *Phys. Rev. Lett.* **118**, 040401 (2017). doi:10.1103/PhysRevLett.118.040401